Characterization of the electron transport and electrical properties in a methanofullerene

L. G. WANG[*], T. X. ZHANG
School of Electrical Engineering and Automation, Henan Polytechnic University, Jiaozuo, 454000, People's Republic of China

The electron transport and electrical properties in a methanofullerene PCBM are investigated. It is demonstrated that the temperature dependent and thickness dependent current density versus voltage characteristics of PCBM devices can be accurately described by using the improved mobility model. In addition, the width of the Gaussian density of states of PCBM is significantly smaller than the values usually reported for conjugated polymers. Furthermore, it is shown that the variation of voltage with boundary carrier density is dependent on the current density. Both the maximum of carrier density and the minimum of electric field appear near the interface of devices.

1. Introduction

Organic solar cells are a promising system for converting solar energy into electricity. These systems are an attractive alternative to inorganic solar cells and have a wide field of applications due to their light weight, low cost, ease of processing, and mechanical flexibility. Conjugated polymer-fullerene bulk-heterojunctions (BHJ) seem to be the most promising candidates for full organic photovoltaic cells [1-3]. Such devices consist of an interpenetrating donor-acceptor network, sandwiched between two electrodes with different work functions to generate an electric field across the organic layer. One of the typical heterojunctions consisting of the conjugated polymer poly (2-methoxy-5-(3',7'-dimethyloctyloxy)-p-phenylene vinylene) (OC_1C_{10}-PPV) as the hole transporting electron donor and the methanofullerene [6,6]-phenyl C_{61}-butyric acid methyl ester (PCBM) as the electron transporting acceptor [1, 4]. Following the ultrafast electron transfer from the conjugated polymer to the fullerene molecules [5], the separated charges are transported via the interpenetrating network to the electrodes and provide voltage for injection into an external circuit.

For the understanding of the optoelectronic properties of OC_1C_{10}-PPV:PCBM-based bulk heterojunction solar cells, it is indispensable to understand the charge transport in the individual components. The hole transport in pure OC_1C_{10}-PPV has been extensively studied due to its application in polymer light-emitting diodes and field-effect transistors [6-9]. On the other hand, the electron transport in PCBM has also been investigated by using the conventional mobility model assuming a Poole–Frenkel type field dependence and neglecting the carrier density dependence [10-13]. However, recently, it was recognized that the mobility μ depends on the electric field E, carrier density p, and temperature T [7, 14, 15]. Based on these results, a full description of the mobility, taking into account both the carrier density and field dependence, was obtained by Pasveer et al. in the form of the extended Gaussian disorder model (EGDM) [8]. However, it should be noted that their model, having a non-Arrhenius temperature dependence $\ln(\mu) \propto 1/T^2$, can only well describe the charge transport at low carrier densities. In order to better describe the charge transport, we proposed an improved model in which the mobility depends on the temperature, carrier density, and electric field based on both the Arrhenius temperature dependence $\ln(\mu) \propto 1/T$ and non-Arrhenius temperature dependence [16]. It has been demonstrated that the improved model can rather well describe the charge transport in organic materials [17-19].

In this paper, the electron transport and electrical properties in methanofullerene [6,6]-phenyl C_{61}-butyric acid methyl ester (PCBM) are investigated. Firstly, we perform a detailed analysis of the current density versus voltage ($J-V$) characteristics for PCBM devices by using the improved mobility model. Subsequently, we calculate and analyze some electrical properties for PCBM, including the variation of $J-V$ characteristics with the boundary carrier density, and the distribution of carrier density and electric field with the distance from the interface.

2. Model

The improved model of the dependence of the mobility μ on the electric field E, carrier density p, and temperature T based on both the Arrhenius temperature dependence and non-Arrhenius temperature dependence can be described as follows [16]:

$$\mu(T, p) = \mu_0(T) \exp[\frac{1}{2}(\hat{\sigma}^2 - \hat{\sigma})(2pa^3)^{\delta}], \quad (1a)$$

$$\mu_0(T) = \mu_0 c_1 \exp(c_2\hat{\sigma} - c_3\hat{\sigma}^2), \quad (1b)$$

$$\delta \equiv 2\frac{\ln(\hat{\sigma}^2 - \hat{\sigma}) - \ln(\ln 4)}{\hat{\sigma}^2}, \quad \mu_0 \equiv \frac{a^2\nu_0 e}{\sigma}, \quad (1c)$$

with $c_1 = 0.48 \times 10^{-9}$, $c_2 = 0.80$, and $c_3 = 0.52$, where $\mu_0(T)$ is the temperature dependent mobility in the limit of zero electric field and charge-carrier density, $\hat{\sigma} \equiv \sigma / k_B T$ is the dimensionless disorder parameter, σ is the width of the Gaussian density of states (DOS), a is the lattice constant, e is the charge of the carriers, and ν_0 is the attempt frequency.

$$\mu(T, p, E) = \mu(T, p)^{g(T,E)} \exp[c_4(g(T,E) - 1)], \quad (2)$$

$$g(T, E) = [1 + c_5(Eea/\sigma)^2]^{-1/2}, \quad (3)$$

where $g(T, E)$ is a weak density dependent function, c_4 and c_5 are weak density dependent parameters, given by

$$c_4 = d_1 + d_2 \ln(pa^3) \quad (4a)$$

$$c_5 = 1.16 + 0.09 \ln(pa^3) \quad (4b)$$

$$d_1 = 28.7 - 36.3\hat{\sigma}^{-1} + 42.5\hat{\sigma}^{-2} \quad (5a)$$

$$d_2 = -0.38 + 0.19\hat{\sigma} + 0.03\hat{\sigma}^2 \quad (5b)$$

Using the above improved model and following coupled equations, the $J - V$ characteristics and other electrical properties of the methanofullerene can be exactly calculated by employing a particular uneven discretization method introduced in our previous papers [20, 21].

$$J = p(x)e\mu(T, p(x), E(x))E(x), \quad (6a)$$

$$\frac{dE}{dx} = \frac{e}{\varepsilon_0 \varepsilon_r} p(x), \quad (6b)$$

$$V = \int_0^L E(x)dx, \quad (6c)$$

where x is the distance from the injecting electrode, L is the methanofullerene layer thickness sandwiched between two electrodes, ε_0 is the vacuum permeability, and ε_r is the relative dielectric constant of the methanofullerene.

3. Results and discussion

Using the improved mobility model and distinctive numerical calculation method as described in section 2, we now perform a systematic study of the electron transport for PCBM. The solution of the coupled equations describing the space-charge limited current (SCLC) with the improved model and the experimental $J - V$ measurements from Ref. [10] for PCBM electron-only devices with various temperatures and various layer thicknesses are displayed in Fig. 1 and Fig. 2, respectively. It can be seen from the figures that the temperature dependent and thickness dependent $J(V)$ curves can be excellently described in the entire range of applied fields only using a single set of parameters, $\sigma = 0.066$ eV, $a = 4.4$ nm, and $\mu_0 = 1550$ m2/Vs. The accurate agreement for the electric field, carrier density, and temperature dependence using a single set of parameters confirms that the improved model is suitable to study the $J - V$ characteristics of PCBM-based devices, and captures the physical essence of the electron transport in PCBM. As for the parameters, it is found that a relatively low a value leads to a relatively low σ value and gives rise to a good description of the experimental $J(V)$ curves only in the low-field and density regime, whereas a relatively high a value leads to a relatively high σ value and gives rise to good fits mainly in the high-field and density regime. The parameter μ_0 decreases with decreasing a and σ, and increases with increasing a and σ. In addition, it is worth noting that the value of the disorder parameter σ is significantly smaller than usually obtained for conjugated polymers [9, 17]. From the same analysis as that applied to the hole mobility of OC$_1$C$_{10}$-PPV, $\sigma = 0.13$ eV, has been reported [9]. The smaller σ of PCBM as compared to OC$_1$C$_{10}$-PPV, demonstrates that the degree of energetic disorder is significantly smaller in PCBM, which gives rise to a higher charge-carrier mobility. For this point, we think that the excellent molecular conformation and strongly ordered stacking of the molecules should be the origin of the higher charge transport properties in PCBM. As a result, the photo-generated electrons in the PCBM are much more mobile than the holes in the OC$_1$C$_{10}$-PPV, making OC$_1$C$_{10}$-PPV:PCBM bulk heterojunction solar cells electron-dominated devices.

As a next step, we further investigate the electrical properties in PCBM devices. The numerically calculated variation of $J - V$ characteristics with the boundary carrier density (the carrier density at the interface) $p(0)$ for PCBM devices with different thicknesses at room temperature is plotted in Fig. 3. The figure shows that the voltage is an increasing function of the current density, and the variation of voltage with $p(0)$ is dependent on the

current density. The voltage decreases with increasing $p(0)$ for relatively small $p(0)$, and also increases with increasing $p(0)$ for sufficiently large $p(0)$. However, in the middle region, the $V - p(0)$ curves are fairly flat, indicating that the voltage is almost independent of $p(0)$ and the $J - V$ characteristics moves into the Ohmic region. In addition, it is clear from the figure that in order to reach the same current density J at the same $p(0)$, the stronger electric field and the corresponding larger voltage are needed in 170 nm thickness device than those in 90 nm thickness device. As for this point, it can also be explained within the framework of the improved mobility model, as the mobility in organic materials is density dependent, the effective mobility as determined in a thick device (with a small average carrier density) is expected to be lower than the mobility as determined in a thin device (with a larger average carrier density). This is consistent with the fact that the thinner devices have the larger concentration of background carriers that have diffused in from the Ohmic contact.

Fig. 3. Theoretical results of voltage versus the boundary carrier density of PCBM devices with thickness 90 nm and 170 nm at room temperature. Different Lines correspond to different current density values
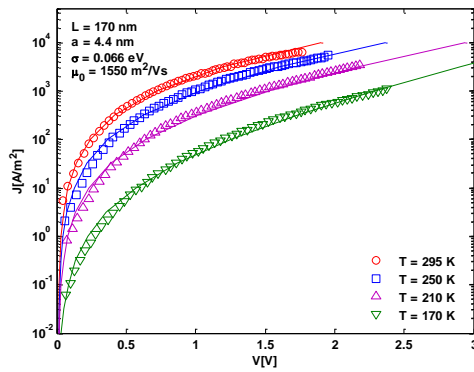

Fig. 1. Temperature dependence of the current density versus voltage characteristics of PCBM device with a layer thickness of 170 nm. Symbols are experimental data from Ref. [10]. Lines are the numerically calculated results from Eqs. (1) – (6)
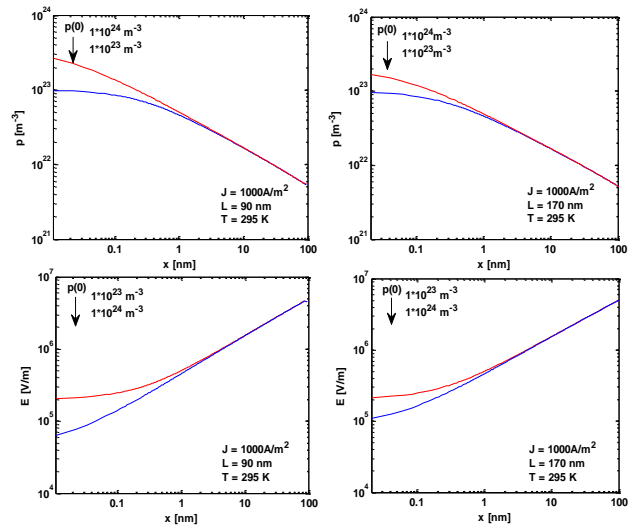
Fig. 4. Numerically calculated distribution of the charge carrier density p and electric field E as a function of the distance x in PCBM devices with thickness 90 nm and 170 nm at room temperature

According to the above analysis of the influence of $p(0)$ on the $J - V$ characteristics, we find that the calculated $J - V$ characteristics are reasonable only when $p(0)$ in the density range of 10^{23}–10^{24}. Thus we take two values of $p(0)$, $(0.1, 1) \times 10^{24}$ m^{-3}, for PCBM devices in the calculations. The numerically calculated results of the carrier density and electric field as a function of the position (the distance from the interface) for PCBM devices are plotted in Fig. 4. It can be seen from the figure that the carrier density $p(x)$ is a decreasing function of the distance x, whereas the electric field $E(x)$ is an increasing function of the distance x. The decrease of the carrier density $p(x)$ for relatively large $p(0)$ is more rapid than that for relatively small $p(0)$. On the other hand, the increase of the electric field $E(x)$ for relatively large $p(0)$ is more rapid than that for relatively small $p(0)$. With the distance x increasing, $p(x)$ rapidly
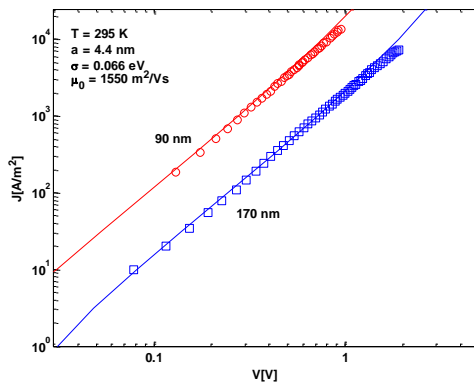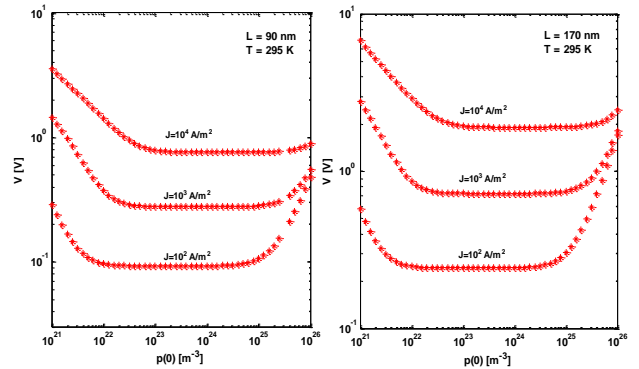

Fig. 2. The current density versus voltage characteristics of PCBM devices with thickness of 90 nm and 170 nm at room temperature. Symbols are experimental data from Ref. [10]. Lines are the numerically calculated results from Eqs. (1) – (6)

reaches saturation. The thickness of accumulation layer is found to decrease with increasing $p(0)$. These results are consistent with the experimental results of Kiguchi et al. [22], and the simulation results of Demeyu and Sven [23]. As a result, the injection of carriers from the electrode into the PCBM layer leads to carriers accumulation near the interface and a decreasing function $p(x)$. The distribution of $p(x)$ leads to the variation of $E(x)$, and the carriers accumulation near the interface results in increasing function $E(x)$.

4. Summary and conclusions

In conclusion, the electron transport and electrical properties in PCBM have been characterized. We demonstrate that the temperature dependent and thickness dependent $J-V$ characteristics of PCBM devices can be accurately described by using the improved mobility model only with a single set of parameter. The width of the DOS $\sigma = 0.066$ eV is significantly smaller than the values reported for OC_1C_{10}-PPV, indicating a low degree of energetic disorder and higher carrier mobility in PCBM. Moreover, it is shown that the effective mobility as determined in a thick device is lower than that in a thin device. The carrier density is found to decrease with increasing the distance, whereas the electric field is found to increase with increasing the distance. These results open the prospect that the improved mobility model is also applicable to the electron transport in a methanofullerene.

References

[1] C. J. Brabec, N. S. Sariciftci, J. C. Hummelen, Adv. Funct. Mater. **11**, 15 (2001).
[2] N. Kaura, M. Singhb, D. Pathakc, T. Wagnerc, J. M. Nunzi, Synth. Met. **190**, 20 (2014).
[3] F. Laquai, D. Andrienko, R. Mauer, P. W. M. Blom, Macromol. Rapid Commun. **36**, 1001 (2015).
[4] S. E. Shaheen, C. J. Brabec, N. S. Sariciftci, F. Padinger, T. Fromherz, J. C. Hummelen, Appl. Phys. Lett. **78**, 841 (2001).
[5] N. S. Sariciftci, L. Smilowitz, A. J. Heeger, F. Wudl, Science **258**, 1474 (1992).
[6] P. W. M. Blom, M. J. M. de Jong, M. G van Munster, Phys. Rev. B **55**, R656 (1997).
[7] C. Tanase, E. J. Meijer, P. W. M. Blom, D. M. de Leeuw, Phys. Rev. Lett. **91**, 216601 (2003).
[8] W. F. Pasveer, J. Cottaar, C. Tanase, R. Coehoorn, P. A. Bobbert, P. W. M. Blom, D. M. deLeeuw, M. A. J. Michels, Phys. Rev. Lett. **94**, 206601 (2005).
[9] L. Wang, H. Zhang, X. Tang, C. Mu, J. Li, Curr. Appl. Phys. **10**, 1182 (2010).
[10] V. D. Mihailetchi, J. K. J. van Duren, P. W. M. Blom, J. C. Hummelen, R. A. J. Janssen, J. M. Kroon, M. T. Rispens, W. J. H. Verhees, M. M. Wienk, Adv. Funct. Mater. **13**, 43 (2003).
[11] J. K. J. van Duren, V. D. Mihailetchi, P. W. M. Blom, T. van Woudenbergh, J. C. Hummelen, R. A. J. Janssen, M. M. Wienk, J. Appl. Phys. **94**, 4477 (2003).
[12] V. D. Mihailetchi, L. J. A. Koster, P. W. M. Blom, C. Melzer, B. de Boer, J. K. J. van Duren, R. A. J. Janssen, Adv. Funct. Mater. **15**, 795 (2005).
[13] M. Lenes, S. W. Shelton, A. B. Sieval, D. F. Kronholm, J. C. Hummelen, P.W.M. Blom, Adv. Funct. Mater. **19**, 3002 (2009).
[14] Y. Roichman, N. Tessler, Synth. Met. **135**, 443 (2003).
[15] C. Tanase, P. W. M. Blom, D. M. de Leeuw, Phys. Rev. B **70**, 193202 (2004).
[16] L. G Wang, H. W. Zhang, X. L. Tang, C. H. Mu, Eur. Phys. J. B **74**, 1 (2010) .
[17] L. G Wang, H. W. Zhang, X. L. Tang, Y. Q. Song, Z. Y. Zhong, Y. X. Li, Phys. Scr. **84**, 045701 (2011).
[18] I. Katsouras, A. Najafi, K. Asadi, A. J. Kronemeijer, A. J. Oostra, L. J. A. Koster, D. M. de Leeuw, P. W. M. Blom, Org. Electron. **14**, 1591 (2013).
[19] L. G Wang, Y. X. Gao, X. L. Liu, L. F. Cheng, J. Optoelectron. Adv. M. **18**(5-6), 504 (2016).
[20] L. G Wang, H. W. Zhang, X. L. Tang, Y. Q. Song, Optoelectron. Adv. Mat. **5**(3), 263 (2011).
[21] M. L. Liu, L. G Wang, J. Optoelectron. Adv. M. **19**(5-6), 406 (2017).
[22] M. Kiguchi, M. Nakayama, T. Shimada, K. Saiki, Phys. Rev. B **71**, 035332 (2005).
[23] L. Demeyu, S. Sven, Phys. Rev. B **76**, 155202 (2007).

_____
*Corresponding author: wangliguo@hpu.edu.cn